

Landfill Settlement with Decomposition and Gas Generation

Ertan Durmusoglu¹; M. Yavuz Corapcioglu, F.ASCE²; and Kagan Tuncay³

Abstract: A one-dimensional multiphase numerical model is developed to simulate the vertical settlement involving liquid and gas flows in a deformable (settling) municipal solid waste (MSW) landfill. MSW is represented by a chemical composition, and a global stoichiometric reaction is used to estimate the maximum yield of gas generation. Following the general assumption accepted in the literature, the gas generated by waste decomposition is assumed to comprise of methane (CH₄) and carbon dioxide (CO₂). The gas generation rate follows an exponentially decaying function of time. The gas generation model developed based on a first-order kinetic single-bioreactor approach includes the governing equations of gas migration, liquid flow, and landfill deformation. The Galerkin finite element method is used to solve the resulting equations. The model developed can be used to estimate the transient and ultimate settlements due to waste decomposition and gas generation in MSW landfills. The proposed model can estimate the waste porosity, gas pressure, liquid pressure, gas saturation, liquid saturation, and stress distributions in settling landfills. The results obtained for a deformable landfill are compared with a landfill having a rigid solid skeleton. Due to settlement, the depth of waste is 27% smaller in deformable landfills than that of the rigid ones.

DOI: 10.1061/(ASCE)0733-9372(2005)131:9(1311)

CE Database subject headings: Landfills; Settlement; Solid wastes; Mathematical models; Waste management; Decomposition; Gas.

Introduction

Goldstein and Madtes (2001) reported that 410 million tons of municipal solid waste (MSW) were generated in the United States in 2000. MSW is a very heterogeneous mixture of wastes that results from municipal functions and services. The mass of waste in landfills is present in three phases: solid, liquid, and gas. The solid phase includes both waste and daily cover soil. The liquid phase consists of infiltrating rainwater during the landfilling processes and the moisture present in wastes at the time of placement. The major source of the gas phase in landfills is gases produced during microbial decomposition of organic waste materials. Landfill gas primarily contains methane (CH₄) (50–60% by volume) and carbon dioxide (CO₂) (40–50%) (Tchobanoglous et al. 1993).

Although the rate of landfilling of waste has dropped from 84 to 61% of the total waste generated over the last decade (Goldstein and Madtes 2001), and other waste treatment options have been developed, landfilling is still considered to be the most common MSW management strategy since it is often the most cost-effective method of waste disposal. In addition, closed

landfills are considered viable sites of land development for numerous purposes such as golf courses, sport fields, wildlife and conservation areas, parking lots, industrial parks, recreational facilities, etc. (Gordon et al. 1986; Magnuson 1999; Conrad 2000). Even a half-century ago, researchers were seeking utilization of landfills for a variety of postclosure land uses (Eliassen 1947). Although landfills are constructed so that future use will not be restricted, many incidents are reported in the literature as case studies related to improperly designed and constructed landfills (e.g., Kelly 1976; Campbell 1996; Eid et al. 2000). The most common problems related with landfills are an assessment of the stability of the waste fill and the control of the gases that result of microbial decomposition.

Landfills are very complex systems in which various interactive processes proceed simultaneously. Gas generation as a result of waste decomposition changes gas and liquid pressures in landfills. These transient changes in liquid and gas pressures may effect porosity, total stress, degree of gas and liquid saturations, and in turn cause deformations, i.e., settlements. These deformations may have negative effects on the integrity of any postclosure structure on the landfill. Unanticipated settlements eventually may result in several problems, such as crack formations in the cover, loss of cover and liner system integrity, and damage to gas and liquid collection and drainage systems. Hence a more accurate prediction of landfill settlement becomes a key issue in the design and construction of landfills.

Settlement in landfills usually occurs in three stages (Sowers 1973; Wall and Zeiss 1995). The first stage is the immediate compression that occurs in direct response to self-weight and/or an external load applied to the waste. Primary compression, i.e., the second stage, is compression due to the dissipation of pore water and gas from the void spaces. This stage may be completed shortly after the waste placement, i.e., within a few months (Sowers 1973; Edil et al. 1990). Sowers (1973) was the first to apply the principles of conventional soil mechanics to estimate the settlement due to the primary compression. The last stage,

¹Assistant Professor, Dept. of Environmental Engineering, Univ. of Kocaeli, Izmit, Kocaeli 41040, Turkey (corresponding author). E-mail: ertan@kou.edu.tr

²Professor, Dept. of Civil Engineering, Texas A&M Univ., College Station, TX 77843. E-mail: yavuz@neo.tamu.edu

³Associate Scientist, Dept. of Chemistry, Indiana Univ., Bloomington, IN 47405. E-mail: ktuncay@indiana.edu

Note. Discussion open until February 1, 2006. Separate discussions must be submitted for individual papers. To extend the closing date by one month, a written request must be filed with the ASCE Managing Editor. The manuscript for this paper was submitted for review and possible publication on May 21, 2003; approved on December 28, 2004. This paper is part of the *Journal of Environmental Engineering*, Vol. 131, No. 9, September 1, 2005. ©ASCE, ISSN 0733-9372/2005/9-1311-1321/\$25.00.

secondary compression, is generally caused by long-term slippages, reorientation of particles, and delayed compression of some waste constituents. This stage can account for a major portion of the total landfill settlement and takes place over many years. The total settlement is then determined as the sum of settlements caused by primary and secondary compressions. Rheological models are also used to predict landfill settlements (Edil et al. 1990). These models were originally developed to predict the settlement of peats, which have compressibility characteristics similar to those of MSW (Berry and Vickers 1975). Yen and Scanlon (1975) developed an empirical relationship to express the settlement rate. Later, Edil et al. (1990) and Ling et al. (1998) applied power and hyperbolic functions to landfill settlement, respectively. The fact that a landfill is an interacting multiphase medium with each phase exhibiting significant spatial and temporal variations makes the above-mentioned approaches more difficult for MSW. In addition, since the contribution of the waste decomposition to long-term settlement can account for a large part of the total settlement, Edgers et al. (1992) and Park and Lee (1997) added the effect of decomposition to the landfill settlement predictions.

Several models have also been developed to address the gas and liquid flow in landfills. The majority of the landfill gas models developed are used to address gas recovery and control. Pressure variations and gas mixtures have been described by the mass conservation law and the equation of state. A homogeneous medium assumption and the application of Darcy's law are common in these models. For these models, refuse is usually divided into three categories having different biodegradability and first-order kinetics (e.g., Findikakis and Leckie 1979; Metcalfe and Farquhar 1987; Arigala et al. 1995). El-Fadel et al. (1996) and Nastev et al. (2001) developed multicomponent gas mixture and heat flow models to predict gas pressure, concentration, and temperature profiles in landfills.

The majority of landfill settlement models focus primarily on a single phase, i.e., gas, liquid, or solid only. As indicated before, a landfill is an interacting multiphase medium with each phase exhibiting significant spatial and temporal variations. Landfill gas and leachate are produced as a result of the physical, chemical, and biological processes within the landfill. Therefore a two-phase modeling approach considering both gas and liquid phases is more representative of a landfill environment. In addition, the organic portion of refuse deposited in landfills is consumed as a result of microbial activities, and the landfill matrix will undergo a time-dependent settlement. To date, there is no published work that simulates gas and liquid flow in deforming and decaying landfills. Recently, El-Fadel and Khoury (2000) reviewed the limitations of the existing MSW landfill models and reported the need of such an integrated model considering the gas, liquid, and solid phases. Therefore, in this study, a multiphase mathematical model is developed for settling landfills. The results were compared with a landfill having a rigid solid skeleton.

Gas Production Model

The microbial decomposition of MSW can be summarized in four phases, namely aerobic phase, anaerobic acid phase, accelerated methane production phase, and decelerated methane production phase (Barlaz et al. 1989). In the first phase, aerobic decomposition takes place with the consumption of O₂ present in the refuse. Organic wastes react with the trapped O₂ to form CO₂, H₂O, biomass, and heat. Upon the depletion of O₂, anaerobic activities

become dominant. In the second phase, carboxylic acids accumulate, and cellulose and hemicellulose decomposition occur. Methane production begins in the accelerated methane production phase and the rate of production decreases in the last phase of decomposition. Anaerobic activities degrade the organic portion, eventually converting the solid organic carbon to CH₄ and CO₂ (Baldwin et al. 1998).

Decomposition of organics provides the source of gas production in landfills, and decomposition products are the primary constituents of landfill gas. The nature of MSW and the stage of decomposition determine the landfill gas composition at any time. The potential of landfill gas production depends on the components of MSW. On the other hand, the gas production rate is influenced by additional factors such as nutrient availability, moisture content, temperature, pH, alkalinity, density of solid waste, particle size, and landfill operation procedures (Barlaz et al. 1989; Senior and Balba 1990). Fresh organic materials represent the necessary substrate supply for bacterial metabolism in landfills (Zehnder and Brock 1979). Degradation of wastes in landfills can be modeled by assuming that microbial transformations are mediated enzymatically and follow Michaleis-Menten kinetics. One of the most widely used approaches for gas generation due to biodegradation of solid waste in a landfill is to employ single-stage first-order kinetics (Hartz and Ham 1982; Wall and Zeiss 1995; Nastev 1998; Nastev et al. 2001). If the rate of gas evolution is given by $-dG_p/dt$, the total gas production rate, α_T , can be expressed as

$$\alpha_T = -\frac{dG_p}{dt} = \frac{dG_c}{dt} \quad (1)$$

where G_p =gas production potential; G_c =cumulative gas production; and t =time. The total gas production rate is proportional to the gas production potential as

$$\alpha_T = \lambda G_p \quad (2)$$

where λ =gas production rate constant. Gas production potential follows exactly the opposite pattern of the cumulative gas production. The sum of the G_p and G_c gives the total capacity for gas production, G_T . The integration of Eq. (1) in the limits for time $t [0; t]$ and for the production potential $G_p [G_T; G_p]$ yields

$$G_p = G_T e^{-\lambda t} \quad (3)$$

If Eq. (2) is employed, the total gas generation rate can be expressed as

$$\alpha_T = \lambda G_T e^{-\lambda t} \quad (4)$$

Since it is assumed that the landfill gas mixture is comprised of CH₄ and CO₂, the total gas generation rate is the sum of the individual gas generation rates.

Since MSW composition varies substantially from region to region, Findikakis and Leckie (1979) suggested that refuse components be categorized into three representative categories according to their biodegradability, each with a corresponding rate constant, λ_m , and gas production potential, G_p^m . That is

$$G_p^m = G_T A_m e^{-\lambda_m t} \quad (5a)$$

Then

$$\alpha_T^m = \sum_i G_T^i A_m \lambda_m e^{-\lambda_m t}, \quad i = 1, 2 \quad (5b)$$

and

Table 1. Waste Components and Corresponding Parameters Considered

Parameter	Waste component		
	Readily degradable	Moderately degradable	Slowly degradable
Fraction of MSW ^a , A_m (kg kg ⁻¹)	0.30	0.45	0.05
Half-life ^b , $t_{1/2}$ (year)	5	30	40
Gas production rate constant ^c , λ_m (year ⁻¹)	0.1386	0.0231	0.0173
Gas production potential ^d , G_p^m (kg m ⁻³)	150.6	225.9	125.5
Total gas production rate ^e , α_T^m (kg m ⁻³ year ⁻¹)	20.8	5.2	2.2

^aEstimated based on the values mentioned by Savage and Diaz (1997).

^bFrom Findikakis and Leckie (1979).

^cCalculated by Eq. (6).

^dCalculated by Eq. (5a).

^eCalculated by Eq. (5b).

$$\alpha_T = \sum_{m=1}^3 \alpha_T^m \quad (5c)$$

where α_T^m =total gas production rate for component m ; m =biodegradability index (1: readily degradable waste, 2: moderately degradable waste, and 3: slowly degradable waste); A_m =fraction of MSW corresponding to component m ; G_p^i =total gas production for gas i (mass of total gas produced per volume of MSW deposited); i =gas index (1: CH₄ and 2: CO₂); and λ_m =gas production rate constant for component m .

In this study, it is assumed that MSW consists of readily, moderately, and slowly degradable wastes and inorganic wastes. The following numbers are used based on the data provided by Savage and Diaz (1997): Readily degradable waste, i.e., food waste (12%), and garden waste (18%), comprises 30% of MSW on a dry weight basis. Moderately degradable waste, i.e., paper products (41%), textiles/leather (1.5%), and wood (2.5%), comprises 45% of MSW. Slowly degradable waste, i.e., plastics/rubber, comprises 5% of MSW. Finally, inorganic waste, i.e., metals, glass, ashes, dirt, and fines, comprises 20% of MSW on a dry weight basis.

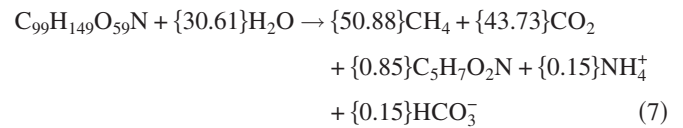
The common procedure for estimation of the gas production rate constant is to employ the half-life concept. The half-life

represents the time ($t_{1/2}$) for which the degradation of one-half of the waste organic matter occurs, i.e., $G_p/G_T=0.5$. If Eq. (3) is employed, the overall rate constant would be

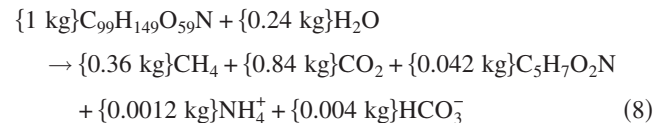
$$\lambda = \frac{-\ln(0.5)}{t_{1/2}} = \frac{0.693}{t_{1/2}} \quad (6)$$

Since the refuse is described as a mixture of three components, each component is characterized by a different degradability and associated half-lives. Table 1 presents the gas production rates, gas production potentials for different biodegradability categories, and calculated gas production rate constants. Landfill gas production rates calculated by Eq. (5c) for these categories with the parameters given in Table 1 are shown in Fig. 1.

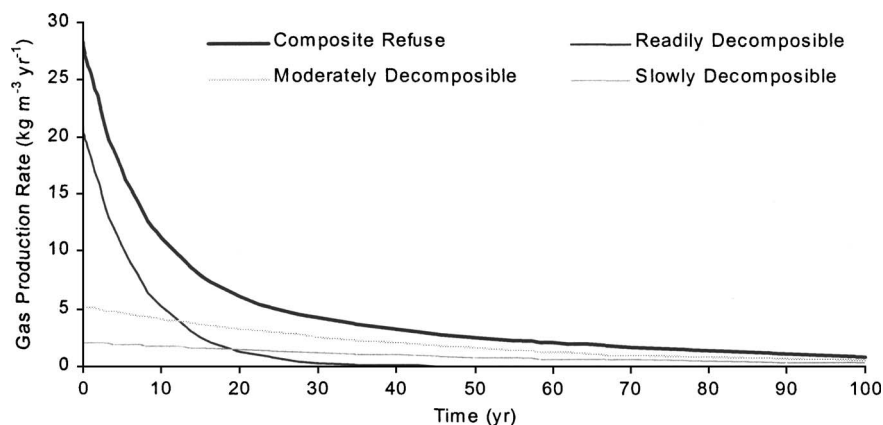
In this study, MSW was represented by an empirical chemical formula, and a global stoichiometric reaction was used for an estimation of the maximum yield. Following Emcon Associates (1980), the empirical formula for average MSW was considered as C₉₉H₁₄₉O₅₉N. Based on landfill density, the amount of gas theoretically produced was predicted employing the method presented by Emcon Associates (1980). Hence the generalized stoichiometric reaction for the overall gas generation can be written as



Moles of CH₄ and CO₂ are determined from Eq. (7) and converted to masses from molecular weights of 16 and 44 g/mol, respectively. Then, the theoretical yield of CH₄ and CO₂ would be



The density of MSW varies within a broad range because its components vary widely (Tchobanoglous et al. 1993). If the average density for the organic fraction of MSW, ρ_o , is known, initial gas production potentials for CH₄ and CO₂, i.e., $G_p^{\text{CH}_4}$ and $G_p^{\text{CO}_2}$, can be estimated by Eq. (8). Based on the resume of the data reported by Nastev (1998), ρ_o is assumed to be 420 kg/m³. Hence, one obtains $G_p^{\text{CH}_4}=0.36 \times 420=150 \text{ kg CH}_4 \text{ per m}^3 \text{ MSW}$,

**Fig. 1.** Gas production rates for different waste categories

and similarly, one obtains $G_p^{CO_2} = 0.84 \times 420 = 352$ kg CO_2 per m^3 MSW. Therefore total potential of gas generation, $G_p (=G_p^{CH_4} + G_p^{CO_2})$, would be 502 kg gas per m^3 MSW. This approach oversimplifies the complex decomposition processes with the various assumptions considered for MSW. For instance, this method does not include any evaluation of the extent of biodegradability of the organic matter. In addition, this gas production estimation assumes optimal anaerobic conditions of moisture, pH, temperature, C/N ratio (weight of carbon divided by the weight of nitrogen), and micronutrients. Implicit in this approach is the absence of toxic substances that would impede the gas generation process. Although these idealized conditions do not exist in most landfills, the results obtained by this approach do put maximum boundaries upon the potential for gas production (Emcon Associates 1980).

Model Development

Although no previous work on landfill deformation incorporating flow models and degradation has been reported, relevant research was published in the area of deformable porous media (e.g., Narasimhan and Witherspoon 1977; Corapcioglu 1979; Schrefler et al. 1995). In this study, it is assumed that decomposition of waste generates a mixture of gas, which in turn causes a change in gas and liquid pressures in the landfill. These processes also affect the porosity, total stress, and the degree of liquid and gas saturations. Finally, the transient change in liquid and gas pressures leads to deformation of the landfill. This deformation implies that the solid particles, as well as the liquid and gas present, are in motion. Due to landfill deformation, Darcy's law should be defined in terms of velocities of liquid and gas relative to solid deformation (Bear 1972; Corapcioglu 1979). The one-dimensional landfill domain is assumed to be comprised of a liquid phase, a gas phase, and a deformable solid matrix with transient gas generation. Both liquid and gas phases are also assumed to be compressible.

The conservation of mass equation for the solid phase can be expressed as

$$-\frac{\partial \rho_b}{\partial t} = \frac{\partial(\rho_b V_s)}{\partial z} + \alpha_T Y \quad (9)$$

where ρ_b = bulk density of solid waste; V_s = solid phase velocity; Y = yield coefficient (mass of solid waste/mass of gas phase); and z = spatial coordinate.

Since the solid phase is comprised of organic and inorganic components, another mass balance equation is required to explain the relationship between these two components, i.e., organic and inorganic. It is assumed that the density of the inorganic component of MSW is constant in space and time. Furthermore, the writers note that, although the organic component of the solid waste undergoes a reduction in mass due to microbial decomposition, and a reduction in volume due to deformation of the solid matrix, the density of the organic component was also assumed to be constant. However, the fractions of individual components vary. As the organic fraction of the waste diminishes with time, the inorganic fraction approaches one (i.e., $s_o + s_i = 1$). That is

$$-\frac{\partial[(1-n)s_o\rho_o]}{\partial t} = \frac{\partial[(1-n)s_o\rho_o V_s]}{\partial z} + \alpha_T Y \quad (10a)$$

and

$$-\frac{\partial[(1-n)s_i\rho_i]}{\partial t} = \frac{\partial[(1-n)s_i\rho_i V_s]}{\partial z} \quad (10b)$$

where n = porosity; s_o = organic fraction of solid waste; s_i = inorganic fraction of solid waste; ρ_o = density of organic portion of solid waste; and ρ_i = density of inorganic portion of solid waste. The sum of the organic and inorganic portions gives the total bulk density of MSW as

$$\rho_b = (1-n)(s_o\rho_o + s_i\rho_i) \quad (11)$$

The conservation of mass for the liquid phase is expressed as

$$-\frac{\partial(\rho_l\theta_l)}{\partial t} = \frac{\partial(\rho_l\theta_l V_l)}{\partial z} \quad (12)$$

where ρ_l = liquid phase density; θ_l = volumetric liquid content expressed as $\theta_l = nS_l$; S_l = liquid phase saturation; and V_l = liquid phase velocity.

In a deforming porous medium, the solid particles, as well as the liquid and gas phases, are in motion. Therefore Darcy's law is expressed in terms of the liquid velocity relative to the deforming solid phase

$$q_{rl} = -\frac{k_{rl}k}{\mu_l} \left(\frac{\partial P_l}{\partial z} - \rho_l g \right) = \theta_l (V_l - V_s) \quad (13)$$

where q_{rl} = specific liquid discharge relative to moving solid; k = permeability; k_{rl} = relative permeability of the liquid phase; P_l = liquid pressure; μ_l = viscosity of the liquid phase; and g = gravitational acceleration.

The compressibility of the liquid phase, β_l , is defined under isothermal conditions as

$$\beta_l = \frac{1}{\rho_l} \frac{\partial \rho_l}{\partial P_l} \quad (14)$$

Integration of Eq. (14) yields the equation of state for the liquid phase

$$\rho_l = \rho_l^o \exp[\beta_l(P_l - P_l^o)] \quad (15a)$$

where ρ_l^o = initial liquid density; and P_l^o = reference liquid pressure. Eq. (20a) can be approximated as

$$\rho_l = \rho_l^o [1 + \beta_l(P_l - P_l^o)] \quad (15b)$$

For incompressible liquids, $\beta_l = 0$ and $\rho_l = \rho_l^o = \text{constant}$.

The conservation of mass equation for the gas phase is given by

$$-\frac{\partial(\rho_g\theta_g)}{\partial t} = \frac{\partial(\rho_g\theta_g V_g)}{\partial z} - \alpha_T \quad (16)$$

where ρ_g = gas mixture density; θ_g = volumetric gas content expressed as $\theta_g = nS_g$; S_g = gas phase saturation; and V_g = gas phase velocity. Similar to the liquid phase, the velocity of the gas phase relative to the deforming solid phase is

$$q_{rg} = -\frac{k_{rg}k}{\mu_g} \left(\frac{\partial P_g}{\partial z} - \rho_g g \right) = \theta_g (V_g - V_s) \quad (17)$$

where q_{rg} = specific gas discharges relative to moving solid; k_{rg} = relative permeability of the gas phase; P_g = gas pressure; and μ_g = viscosity of the gas phase. The equation of state for the gas phase is expressed by the ideal gas law

$$P_g = \frac{\rho_g}{M_g} \bar{R} \Phi \quad (18)$$

where M_g =molecular weight of gas mixture; \bar{R} =universal gas constant; and Φ =absolute temperature. Under isothermal conditions, Eq. (18) becomes

$$\frac{d\rho_g}{dP_g} = \rho_g^o \frac{1}{P_g^o} \quad (19a)$$

where ρ_g^o =initial gas mixture density; and P_g^o =reference gas pressure. Eq. (19a) can also be expressed as

$$\rho_g = \rho_g^o \frac{P_g}{P_g^o} \quad (19b)$$

The density and the molecular weight of the gas mixture can be estimated by

$$\rho_g = \sum_i y_i \rho_g^i, \quad i = 1, 2 \quad (19c)$$

and

$$M_g = y_i M_i + y_j M_j \quad (19d)$$

where ρ_g^i =density of gas i ; y_i , y_j =mole fractions of gas i and gas j ; and M_i , M_j =molecular weights of gas i and gas j .

The viscosity of the gas mixture can be expressed as a function of the viscosities of individual gases (Reid et al. 1987)

$$\mu_g = \sum_{i=1} \frac{\mu_i}{1 + \sum_{j=1, j \neq i} \varphi_{ij} \frac{y_j}{y_i}} \quad (20a)$$

and

$$\varphi_{ij} = \frac{\left[1 + \left(\frac{\mu_i}{\mu_j} \right)^{1/2} \left(\frac{M_j}{M_i} \right)^{1/4} \right]^2}{\sqrt{8} \left(1 + \frac{M_i}{M_j} \right)^{1/2}} \quad (20b)$$

where μ_i , μ_j =viscosities of gas i and gas j .

The following empirical expressions (Reid et al. 1987) can be employed to calculate the viscosities of CH₄ and CO₂ at a particular temperature (in Kelvin)

$$\mu_{\text{CH}_4} = (1.935 + 0.0305\Phi) \times 10^{-6} \quad [\text{N s m}^{-2}] \quad (20c)$$

and

$$\mu_{\text{CO}_2} = (-30.212 + 0.256\Phi - 0.00035\Phi^2) \times 10^{-6} \quad [\text{N s m}^{-2}] \quad (20d)$$

Municipal solid waste is a porous medium with pore spaces between irregularly shaped solid grains. Sarsby (2000) presents several expressions relating the permeability to the solid matrix properties. Most of these expressions are empirical and relate to uniform granular materials. Such relationships therefore have limited applications to MSW having a wide range of particle sizes. However, due to the lack of an expression relating the permeability to the properties of MSW, and being one of the most widely used expressions (Bear 1972), the Kozeny-Carman equation is employed. That is

$$k = k_o \frac{n^3}{(1-n)^2} \quad (21)$$

where k_o =reference permeability.

Since the voids in MSW are not completely filled by the liquid phase, the presence of the gas phase reduces the volume of medium available for liquid flow in an unsaturated medium. When the gas and liquid phases flow together through a porous medium, saturations of the phases are less than unity ($S_l + S_g = 1$). Relative permeability is the ratio of the corresponding effective permeability to the permeability of the porous medium. The relative permeabilities are difficult to predict, particularly in materials with changing properties such as MSW. In this study, the relationships proposed by Brooks and Corey (1966) are used. That is

$$k_{rl} = \frac{k_l}{k} = \left(\frac{S_l - S_r}{S_m - S_r} \right)^3 \quad (22a)$$

and

$$k_{rg} = \frac{k_g}{k} = \left(1 - \frac{S_l - S_r}{S_m - S_r} \right)^3 \quad (22b)$$

where k_l =permeability of liquid phase; k_g =permeability of gas phase; S_r =residual saturation; and S_m =maximum saturation.

Several expressions for the capillary pressure are available in the literature. Among them, the empirical power law, originally developed for soils, expresses the capillary pressure as a function of water saturation (Clapp and Hornberger 1978)

$$\frac{P_c}{\gamma_w} = \Psi_s \left(\frac{\theta_l}{\theta_s} \right)^{-\eta} \quad (23)$$

where P_c =capillary pressure; Ψ_s =saturation suction head; θ_s =saturation volumetric moisture content; γ_w =unit weight of water; and η =fitting parameter.

Korfatis et al. (1984) applied the power law equation to experimental data obtained from MSW samples. The saturation suction head was determined to be 6.2 cm of water. Measurements of the saturated moisture content ranged from 50 to 60%, and 55% was recommended for use when data are not available. The field capacity was determined experimentally to vary from 20 to 30%. The fitting parameter, η , was determined to be 1.5. However, model calibration to predict leaching from a large-scale column led to a different value for η , i.e., 4.0. The channeling effect in large-scale columns was the main reason for this observed difference.

Since MSW is not an elastic solid matrix in a theoretical sense, a viscoelastic approach was employed to incorporate the time-dependent deformation of the solid matrix, i.e., the Maxwell's body rather than a Hookean spring. Fig. 2 presents the Maxwell's body consisting of two basic elements joined in series, namely the Hookean spring, characterized by its compressibility, and a dashpot, characterized by its viscosity (Suklje 1969). Yoshikuni et al. (1994) stated that Maxwell's body explains the secondary compression phenomena best among other rheological considerations. Therefore the rate of strain is defined as

$$\frac{\partial \epsilon}{\partial t} = m_v \frac{\partial \sigma'}{\partial t} + \frac{1}{\kappa} \sigma' \quad (24)$$

where ϵ =strain; m_v =coefficient of volume change; σ' =effective stress; and κ =bulk viscosity of the solid waste. Here, m_v is defined by

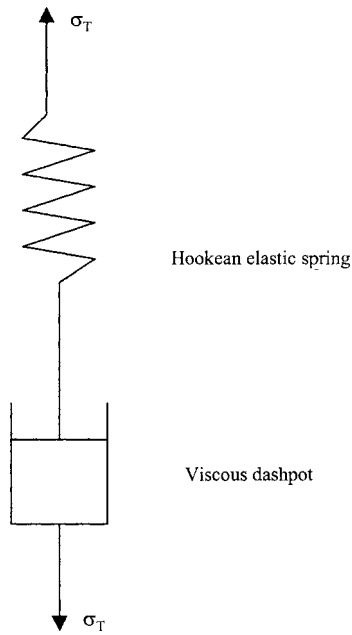


Fig. 2. Schematic representation of Maxwell's body

$$m_v = \frac{(1 + \nu)(1 - 2\nu)}{E(1 - \nu)} \quad (25a)$$

and σ' can be expressed as below following Fredlund and Rahardjo (1993)

$$\sigma' = \sigma_T + S_l P_l + S_g P_g \quad (25b)$$

where ν =Poisson's ratio; E =elastic (or Young's) modulus; and σ_T =total stress (compressive stresses are assumed to be negative). The total stress in a MSW column can be calculated as

$$\sigma_T = - \int_{\text{bottom}}^{\text{top}} (\theta_l \rho_l + \theta_g \rho_g + \rho_b) g dz \quad (26)$$

Numerical Solution

The Galerkin finite element method is employed to discretize the governing partial differential equations. The Galerkin method is the most popular one among the other finite element methods in subsurface flow and transport models. Instead of solving the resulting discretized nonlinear algebraic equations, the writers adopted a technique that is easy to implement and efficient for one-dimensional problems. The technique developed linearizes the nonlinear algebraic equations and checks the mass error committed as a result of this linearization. Then, this mass error is used to control the time-step during the simulations. Finally, the resulting equations are solved by the Gaussian elimination technique. The reader is referred to Durmusoglu (2002) for a detailed presentation of the numerical solution.

The mass balance equations for the liquid and gas phases can be written as

$$n S_l \rho_l \beta_l \frac{\partial P_l}{\partial t} + \rho_l n \frac{\partial S_l}{\partial t} + \rho_l S_l \frac{\partial V_s}{\partial z} + \rho_l S_l \frac{\alpha_T Y}{\rho_o} = \frac{\partial}{\partial z} \left[\frac{\rho_l k_l}{\mu_l} \left(\frac{\partial P_l}{\partial z} - \rho_l g \right) \right] \quad (27a)$$

and

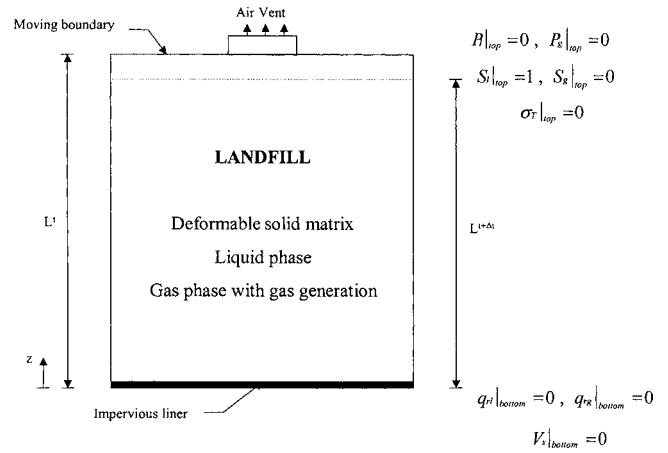


Fig. 3. Idealized landfill with boundary conditions employed

$$n(1 - S_l) \frac{M_g}{R\Phi} \frac{\partial P_g}{\partial t} - \rho_g n \frac{\partial S_l}{\partial t} + \rho_g (1 - S_l) \frac{\partial V_s}{\partial z} + \alpha_T \left(\frac{Y \rho_g (1 - S_l)}{\rho_o} - 1 \right) = \frac{\partial}{\partial z} \left[\frac{\rho_g k_g}{\mu_g} \left(\frac{\partial P_g}{\partial z} - \rho_g g \right) \right] \quad (27b)$$

Discretization of Eqs. (27a) and (27b), along with the capillary pressure, i.e., $P_c = P_g - P_l$, constitute the discretized equations for three unknowns, i.e., $P_l^{t+\Delta t}$, $P_g^{t+\Delta t}$, $S_l^{t+\Delta t}$, and three equations (Durmusoglu 2002). This is basically a two-phase system comprised of gas and liquid phases. In addition, Eqs. (27a) and (27b) include the solid phase velocity and the gas generation terms. The solid velocity term can be replaced by the rate of strain. Here, before solving the system of equations, the gas generation term is incorporated into the program. After the system of equations is solved for $P_l^{t+\Delta t}$, $P_g^{t+\Delta t}$, $S_l^{t+\Delta t}$, and $S_g^{t+\Delta t}$, the total stress is calculated by integrating the average density, along with the landfill thickness, as given in Eq. (26). Then, the new values for the porosity and rate of strain are obtained to determine the new nodal coordinates, which in turn give the amount of deformation. Discretization of the porosity term yields

$$n^{t+\Delta t} = n^t + \left\{ (1 - n^{t+\Delta t}) \left[m_v \left(\frac{\sigma_T^{t+\Delta t} - \sigma_T^t}{\Delta t} + \frac{\bar{P}^{t+\Delta t} - \bar{P}^t}{\Delta t} \right) + \frac{1}{\kappa} (\sigma_T^{t+\Delta t} + \bar{P}^{t+\Delta t}) \right] + \frac{\alpha_T Y}{\rho_o} \right\} \Delta t \quad (28)$$

where superscripts t and $t+\Delta t$ denote the current time t and the future time with an increment of Δt , respectively. Here, $\bar{P} = S_l P_l + S_g P_g$. The rate of strain can be expressed as

$$\frac{\partial \epsilon}{\partial t} = \left(\frac{dn}{dt} - \frac{\alpha_T Y}{\rho_o} \right) \frac{1}{(1 - n)} \quad (29)$$

As a result, the new element spacing is obtained from

$$\Delta z^{t+\Delta t} = \frac{1}{1 - \epsilon} \Delta z^t \quad (30)$$

Initially, the landfill is assumed to be liquid saturated to represent the worst-case scenario for maximum degradation. Hence the pressure distribution becomes hydrostatic throughout the landfill. In addition, it is assumed that the rate of strain is

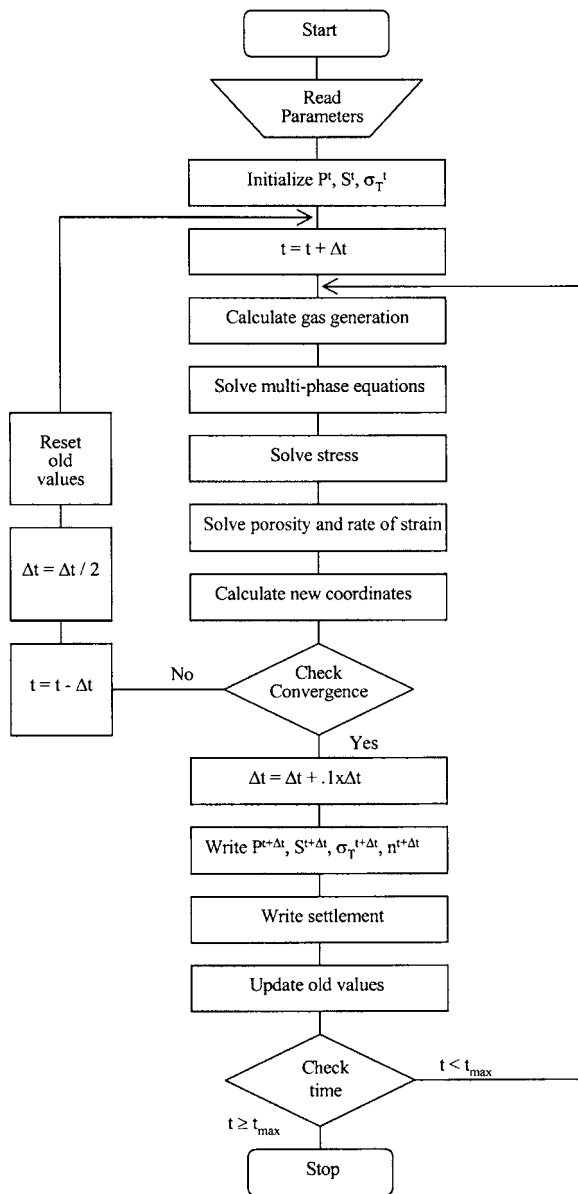


Fig. 4. Flow diagram indicates the operational sequence

initially zero in the domain. Therefore the initial conditions considered in the model for the pressures, degree of saturations, and the total stress are as follows:

$$P_l|_{t=0} = \rho_l g(L_o - z) \quad (31a)$$

$$P_g|_{t=0} = P_l|_{t=0} \quad (31b)$$

$$S_l|_{t=0} = 1 \quad (31c)$$

$$\sigma_T|_{t=0} = -(n\rho_l + \rho_b)g(L_o - z) \quad (31d)$$

where L_o = initial height of landfill.

An idealized landfill with boundary conditions employed is given in Fig. 3. After discretization, the flow diagram shown in Fig. 4 and the parameters given in Table 2 are incorporated into a computer program. As depicted in the flow diagram, the parameters are inputted and the gas generation is calculated. After the multiphase equations, stress, porosity, and the rate of strain are solved, new coordinates are calculated. During the simulation,

Table 2. Model Parameters

Parameter	Value
Reference porosity ^a , n_o	0.4
Reference permeability ^b , k_o (m ²)	1×10^{-11}
Bulk viscosity of MSW ^c , κ (Pa s)	1×10^{12}
Coefficient of compressibility ^d , m_v (Pa ⁻¹)	1×10^{-7}
Average solid waste bulk density ^e , ρ_b (kg m ⁻³)	1,000
Inorganic fraction of MSW ^f , s_i	0.2
Organic fraction of MSW ^f , s_o	0.8
Reference gas mixture density ^g , ρ_g^o (kg m ⁻³)	1.1317
Gas mixture molecular weight ^h , M_g (kg mol ⁻¹)	0.029
Gas mixture viscosity ⁱ , μ_g (Pa s)	1.4×10^{-5}
Residual liquid saturation ^c , S_r	0.0375
Saturation suction head ^j , ψ_s (m)	0.062
Liquid compressibility ^k , β_l (Pa ⁻¹)	0.5×10^{-9}
Liquid viscosity ^k , μ_l (Pa s)	1×10^{-3}
Reference liquid density ^k , ρ_l^o (kg m ⁻³)	994.13
Absolute temperature ^b , Φ (K)	308
Universal gas constant, \bar{R} (N m mol ⁻¹ K ⁻¹)	8.31441
Gravitational acceleration, g (m s ⁻²)	9.81

^aValue is within the range mentioned by Oweis et al. (1990).

^bValue is within the range mentioned by Tchobanoglous et al. (1993).

^cValue is within the range mentioned by Yoshikuni et al. (1995).

^dFrom Marques et al. (2003).

^eReported by Nastev (1998).

^fEstimated based on the values mentioned by Savage and Diaz (1997).

^gEstimated by Eq. (19c).

^hEstimated by Eq. (19d).

ⁱEstimated by Eq. (20a) and (20b).

^jFrom Korfiatis et al. (1984).

^kProperty of water.

the residual error introduced by the linearization of the nonlinear mass balance equations is calculated and checked with a specified tolerance after the coefficient matrices are constructed and the equations are solved. Therefore the time step is adjusted due to the residual error. If the residual error is more than the predetermined tolerance, the time step is subtracted from the current time, divided by two, and the parameters are reset; otherwise, it is increased by 10%, the parameters with new values are written, and the settlement is calculated.

Results and Discussions

A one-dimensional landfill is initially divided into elements with equal sizes. During each time step, the size of the elements is adjusted to consider the change in height of the landfill due to settlements caused by the decomposition and the overburden pressure. Since typical reported landfill heights are between 15 and 25 m (Tchobanoglous et al. 1993), a 15-m-high landfill is considered to describe the basic characteristics of deformable and rigid landfills. The landfill is divided into 20 elements of equal size, i.e., $\Delta z = 0.75$ m. The simulation results are obtained for times, 10, 30, 50, and 100 years.

Fig. 5 shows the gas and liquid pressure spatial profiles for a deformable landfill at selected times. Similar pressure profiles vary linearly with landfill height and are obtained for both gas and liquid phases. While the gas pressure is 140 kPa at the bottom at

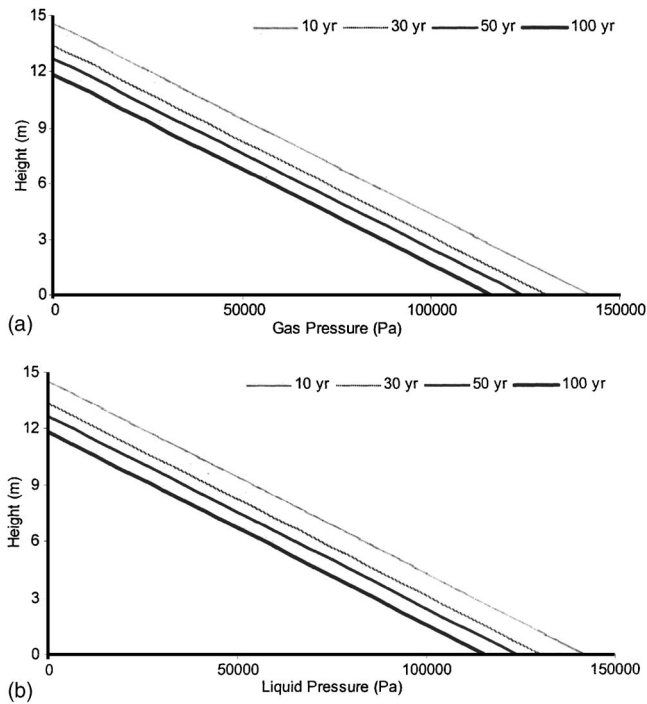


Fig. 5. (a) Gas and (b) liquid pressure spatial profiles for a deformable landfill at selected times

10 years, it is reduced to 125 kPa in 50 years. The reduction in gas pressure is due to the reduction in the gas production potential of the waste with time. In the vertical direction, the highest pressure is observed at the landfill bottom, i.e., 140 kPa. This is a relatively high pressure buildup. Gas pressure is strongly dependent on the gas production potential and the waste permeability. In this particular case, since it is assumed that the waste is deposited at one time rather than in increments, and the landfill gas production is uniform throughout the depth, such pressure increases are expected. In addition, the permeability adjustments for porosity changes contribute significantly to the pressure increase. Following the high buildup in the early years, gas pressure decreases to 115 kPa at 100 years with a pressure reduction of 25 kPa. As mentioned before, the air vent at the top of the landfill allows for the complete release of gas generated to the atmosphere.

The gas and liquid saturation spatial profiles for a deformable landfill at selected times are illustrated in Fig. 6. Due to the high gas production, the gas saturation is high in early years. Later, the gas saturation decreases and approximately half of the saturation reduction occur in 100 years at the landfill bottom. The saturation profiles are highly affected by the boundary conditions assumed for the model solution. Since the landfill surface is assumed saturated by the liquid phase, the gas saturation is always zero at the top. Moreover, this assumption causes the differences between gas saturations at the top and the bottom of the landfill. Since the sum of the gas and the liquid saturations is always equal to one, i.e., $S_l + S_g = 1$, exactly opposite saturation profiles are obtained in a particular time and height.

Fig. 7(a) shows the total stress profile for a deformable landfill at selected times. Similar to the pressure profiles, the total stress is decreased with time due to the waste decomposition. The mass loss and the pressure reduction lead to a reduction in the average landfill density over time. The total density is calculated by Eq. (26) by integrating the total mass in the z direction.

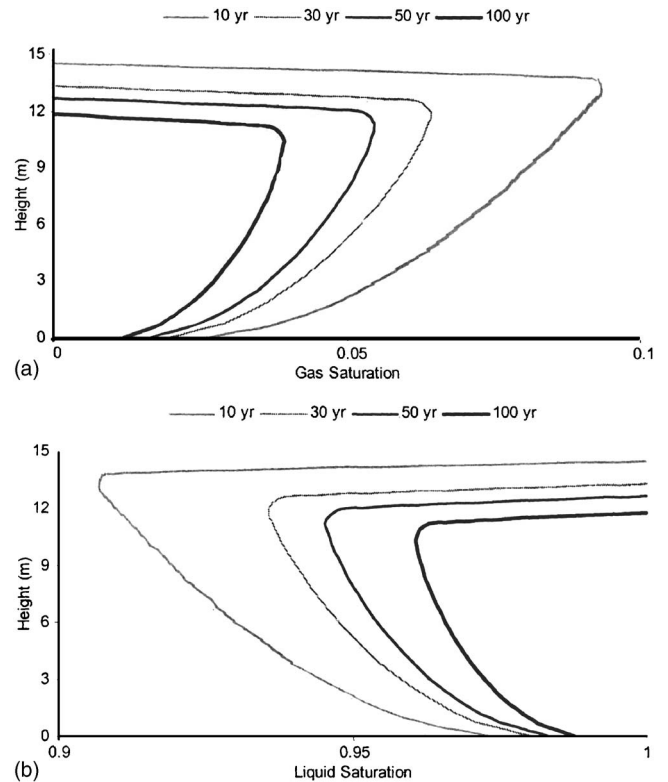


Fig. 6. (a) Gas and (b) liquid saturation spatial profiles for a deformable landfill at selected times

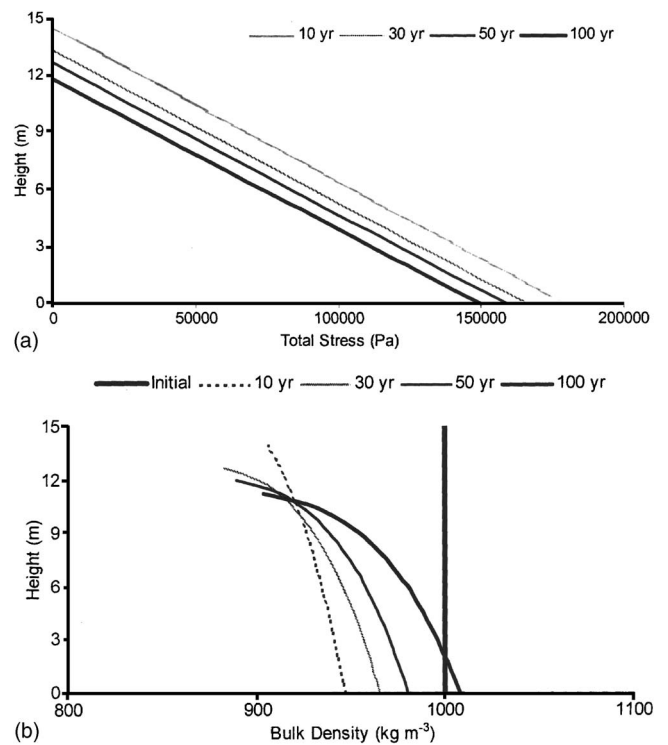


Fig. 7. (a) Total stress and (b) bulk density spatial profiles for a deformable landfill at selected times

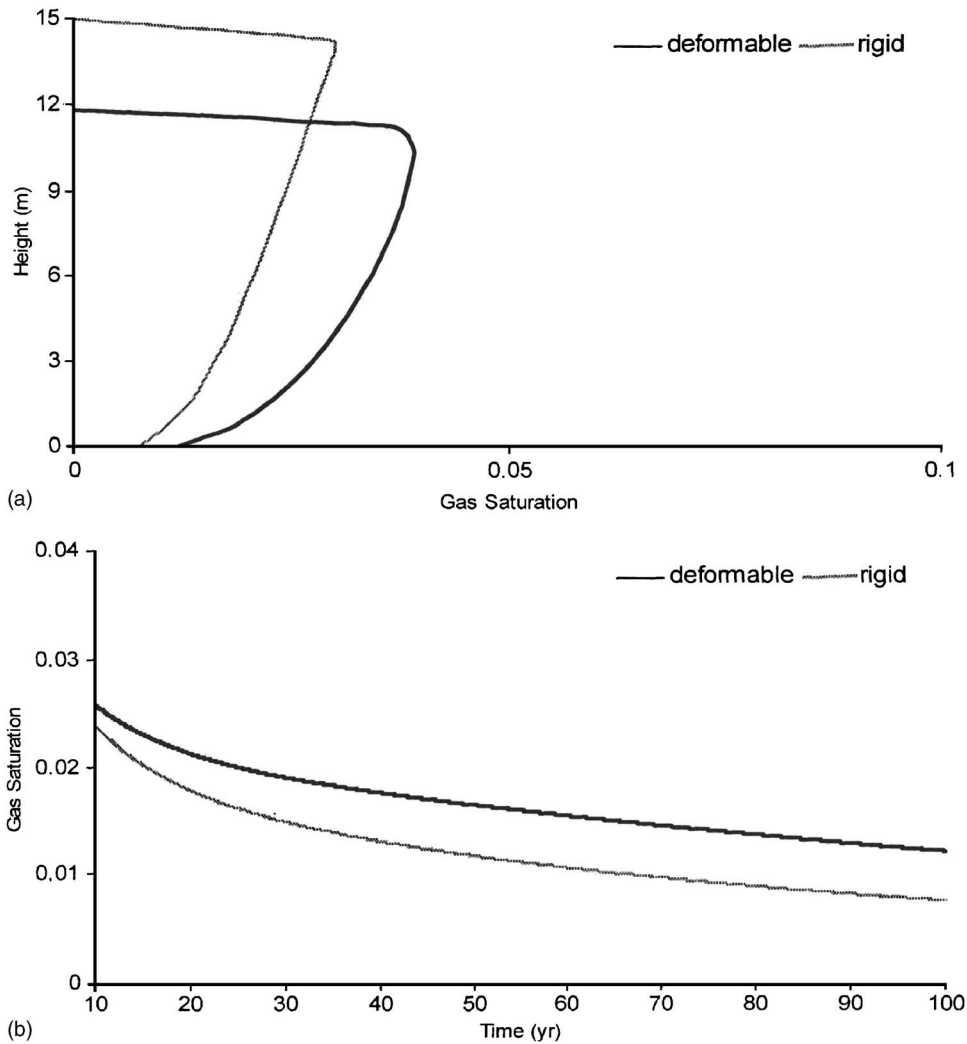


Fig. 8. (a) Gas saturation spatial profiles for deformable and rigid landfills at 100 years and (b) gas saturation temporal profiles at the bottom for deformable and rigid landfills

The density reduction has a significant contribution in the total stress reduction in the early years. In the later years, although the density is increased as the result of the settlement [see Fig. 7(b)], the total stress is continued to decrease due to the increase in gas and liquid pressures. The total stress at the bottom of the landfill is reduced from 180 to 150 kPa in 100 years. Since it is assumed that there is no overburden pressure at the landfill surface, the total stress is zero. Fig. 7(b) presents the spatial bulk density profiles for a deformable landfill. Initial bulk density of $1,000 \text{ kg m}^{-3}$ is decreased in the early years, e.g., 10 years, due to the mass reduction as the result of waste decomposition. In the later years, the bulk density is increased due to landfill settlement.

The results obtained for a deformable landfill are compared with a 15-m-high rigid landfill. The same model parameters used in the deformable landfill are also employed for the rigid landfill except for the coefficients of volume change, m_v , and the bulk viscosity, κ , which are both identified as major parameters in landfill deformation. To represent a rigid landfill, relatively small m_v , e.g., $1 \times 10^{-25} \text{ Pa}^{-1}$, and relatively large κ , e.g., $1 \times 10^{25} \text{ Pa s}$, values were employed. Fig. 8(a) shows the gas saturation spatial profiles for deformable and rigid landfills at 100 years. The gas saturation at a certain height is always lower in a rigid landfill than in a deformable one. This is caused by the settlement taking

place in the deformable landfill. Fig. 8(b) presents the gas saturation temporal profile at the bottom for deformable and rigid landfills. The effect of settlement on the gas saturation is more obvious in the temporal distribution.

There is a 30 kPa difference between the total stress distributions in the rigid and deformable landfills at 100 years as shown in Fig. 9(a). Although the gas generation decreases with time, the overburden pressure in the rigid landfill remains approximately the same due to the rigid solid matrix. On the other hand, the total stress decreases with time due to the settlement in a deformable landfill. A 27% difference in height is observed between the results obtained by deformable and rigid landfills at all stress levels.

Fig. 9(b) presents the settlement profile for a deformable landfill. The height of the landfill is reduced by 22% in 100 years. The reduction is due to the settlement taking place after the waste is deposited in the landfill. The waste decomposition and the total stress are the primary factors causing the settlement. The total stress drives the substantial long-term settlement. In the literature, several researchers reported total settlements reaching 20–50% of the initial landfill depth (e.g., Stearns 1987; Tchobanoglous et al. 1993). Wall and Zeiss (1995) also reported that the contribution of waste decomposition accounts for a large portion of the settlement, i.e., about 40% of the initial depth. In this study, a slower

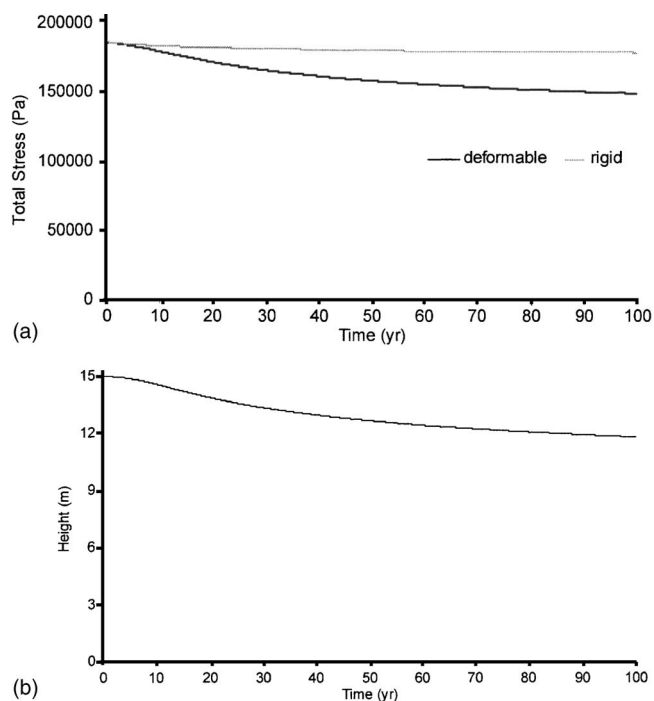


Fig. 9. (a) Total stress temporal profiles at the bottom for deformable and rigid landfills and (b) settlement profile for a deformable landfill

settlement rate is observed in the early years, i.e., less than 10 years. The lack of high initial compression is due to the Maxwell model employed for the compression of MSW. The high gas pressure buildup delays the settlement of the landfill until the gas production potential is sufficiently reduced. Whenever the total stress overcomes the pressure buildup, the settlement rate increases, reaching steady state at around 80 years.

Conclusions

A multiphase mathematical model is developed to simulate fluid flows in a deformable MSW landfill. It is assumed that a gas mixture is generated as a result of decomposition processes in the landfill. The gas generation affects the gas and liquid pore pressures as well as various landfill parameters, e.g., porosity, total stress, liquid and gas saturations, permeabilities, and total stress. Previously, various mathematical models were developed to simulate liquid and gas flows in landfills (e.g., Findikakis and Leckie 1979; Metcalfe and Farquhar 1987; Arigala et al. 1995; El-Fadel et al. 1996; Nastev et al. 2001). These models assume the landfill is a rigid medium. In this study, the same input parameters were employed to the model developed for two different landfills, namely deformable and rigid. It can be concluded that the modeling of the fluid flows under deformable landfill conditions produces results quite different from that of the rigid landfills. Based on the results, it can be concluded that landfill models for future use should incorporate both landfill deformation and gas generation for more realistic landfill conditions.

The results obtained in this study are for hypothetical cases. Real-world landfill systems were idealized by introducing various assumptions such as initial liquid saturation. Although this assumption may not necessarily represent the reality existing in the field, it represents the worst-case scenario for maximum degradation. An idealized landfill with excess gas pressure

dissipation only at the top boundary was considered for a case with simpler boundary conditions. In addition, the employment of an impervious liner as a boundary condition is one of the limitations of the model. In estimation of gas production, the methane yield used is a theoretical one that serves as the maximum limit for methane production and it is based on the assumptions of the most favorable environmental conditions that can exist for bacterial well-being and complete conversion of the organic fraction which implies optimum conditions. The simplicity achieved with these assumptions justifies their use to investigate the relative importance of certain mechanisms such as gas and liquid flow in deforming and decaying landfills which were studied for the first time in this study.

References

- Arigala, S. G., Tsotsis, T. T., Webster, I. A., Yortsos, Y. C., and Kattapuram, J. J. (1995). "Gas generation, transport, and extraction in landfills." *J. Environ. Eng.*, 121(1), 33–44.
- Baldwin, T. D., Stinson, J., and Ham, R. K. (1998). "Decomposition of specific materials buried within sanitary landfills." *J. Environ. Eng.*, 124(12), 1193–1202.
- Barlaz, M. A., Schaefer, D. M., and Ham, R. K. (1989). "Bacterial population development and chemical characteristics of refuse decomposition in a simulated sanitary landfill." *Appl. Environ. Microbiol.*, 55(1), 55–65.
- Bear, J. (1972). *Dynamics of fluids in porous media*, Dover, New York.
- Berry, P. L., and Vickers, B. (1975). "Consolidation of fibrous peat." *J. Geotech. Eng. Div., Am. Soc. Civ. Eng.*, 101(8), 741–753.
- Brooks, R. N., and Corey, A. T. (1966). "Properties of porous media affecting fluid flow." *J. Irrig. Drain. Div.*, 92(2), 61–88.
- Campbell, D. J. (1996). "Explosion and fire hazards associated with landfill gas." *Landfilling of waste: Biogas*, T. H. Christensen et al., eds., E&FN Spon, London, 133–142.
- Clapp, R. G., and Hornberger, G. M. (1978). "Empirical equations for some soil hydraulic properties." *Water Resour. Res.*, 14(4), 601–604.
- Conrad, L. G. (2000). "A Canadian perspective—Use of the Britannia sanitary landfill site as a golf course." *Proc., 5th Annual Landfill Symp.*, Solid Waste Association of North America, Austin, Tex., 73–79.
- Corapcioglu, M. Y. (1979). "Diffusion of dissolved gas in consolidating porous media." *Water Resour. Res.*, 15(3), 563–568.
- Durmusoglu, E. (2002). "Municipal landfill settlement with refuse decomposition and gas generation." PhD dissertation, Texas A&M Univ., College Station, Tex.
- Edgers, L., Noble, J. J., and Williams, E. (1992). "A biological model for long term settlement in landfills." *Proc., Mediterranean Conf. on Envir. Geotechnol.*, M. A. Usmen and Y. B. Acar, eds., Balkema, Rotterdam, the Netherlands, 177–184.
- Edil, T. B., Ranguette, V. J., and Wuellner, W. W. (1990). "Settlement of municipal refuse." *Geotechnics of waste fills—Theory and practice*, A. Landva and G. D. Knowles, eds., STP No. 1070, ASTM, Philadelphia, 225–239.
- Eid, H. T., Stark, T. D., Evans, W. D., and Sherry, P. E. (2000). "Municipal solid waste slope failure. I: Waste and foundation soil properties." *J. Geotech. Geoenviron. Eng.*, 126(5), 397–407.
- El-Fadel, M., Findikakis, A. N., and Leckie, J. O. (1996). "Numerical modelling of generation and transport of gas and heat in sanitary landfills. I: Model formulation." *Waste Manage. Res.*, 14(5), 483–504.
- El-Fadel, M., and Khoury, R. (2000). "Modeling settlement in MSW landfills: A critical review." *Crit. Rev. Envir. Sci. Technol.*, 30(3), 327–361.
- Eliassen, R. (1947). "Housing construction on refuse landfills." *Eng. News-Rec.*, 138, 756–760.

- Emcon Associates. (1980). *Methane generation and recovery from landfills*, Ann Arbor Science, Ann Arbor.
- Findikakis, A. N., and Leckie, J. O. (1979). "Numerical simulation of gas flow in sanitary landfills." *J. Environ. Eng. Div. (Am. Soc. Civ. Eng.)*, 105(5), 927–945.
- Fredlund, D. G., and Rahardjo, H. (1993). *Soil mechanics for unsaturated soils*, Wiley-Interscience, New York.
- Goldstein, N., and Madtes, C. (2001). "The state of garbage in America." *BioCycle*, 42(12), 42–54.
- Gordon, D. L., Lord, J. A., and Twine, D. (1986). "The Stockley Park project." *Proc., Institution of Civil Engineers Conf.: Building on Marginal and Derelict Land*, Thomas Telford, London, 359–379.
- Hartz, K. E., and Ham, R. K. (1982). "Gas generation rates of landfill samples." *Conserv. Recycl.*, 5(2/3), 133–147.
- Kelly, W. E. (1976). "Ground-water pollution near a landfill." *J. Environ. Eng. Div. (Am. Soc. Civ. Eng.)*, 102(6), 1189–1199.
- Korfiatis, G. P., Demetropoulos, A. C., Bourodimos, E. L., and Nawy, E. G. (1984). "Moisture transport in a solid waste column." *J. Environ. Eng.*, 110(4), 780–796.
- Ling, H. I., Leshchinsky, D., Mohri, Y., and Kawabata, T. (1998). "Estimation of municipal solid waste landfill settlement." *J. Geotech. Geoenviron. Eng.*, 124(1), 21–28.
- Magnuson, A. (1999). "Landfill closure: End uses." *MSW Manage.*, 9(5), 1–8.
- Marques, A. C. M., Filz, G. M., and Vilar, O. M. (2003). "Composite compressibility model for municipal solid waste." *J. Geotech. Geoenviron. Eng.*, 129(4), 372–378.
- Metcalfe, D. E., and Farquhar, G. J. (1987). "Modeling gas migration through unsaturated soils from waste disposal sites." *Water, Air, Soil Pollut.*, 32, 247–259.
- Narasimhan, T. N., and Witherspoon, P. A. (1977). "Numerical model for saturated-unsaturated flow in deformable porous media. 1: Theory." *Water Resour. Res.*, 13(3), 657–664.
- Nastev, M. (1998). "Modeling landfill gas generation and migration in sanitary landfills and geological formations." PhD dissertation, Laval Univ., Quebec, Canada.
- Nastev, M., Therrien, R., Lefebvre, R., and Gelinias, P. (2001). "Gas production and migration in landfills and geological materials." *J. Contam. Hydrol.*, 52, 187–211.
- Oweis, I. S., Smith, D. A., Ellwood, R. B., and Greene, D. S. (1990). "Hydraulic characteristics of municipal refuse." *J. Geotech. Eng.*, 116(4), 539–553.
- Park, H. I., and Lee, S. R. (1997). "Long-term settlement behavior of landfills with refuse decomposition." *J. Solid Waste Technol. Manage.*, 24(4), 159–165.
- Reid, R. C., Prausnitz, J. M., and Poling, B. E. (1987). *The properties of gases and liquids*, McGraw-Hill, New York.
- Sarsby, R. (2000). *Environmental geotechnics*, Thomas Telford, London.
- Savage, G. M., and Diaz, L. F. (1997). "Solid waste characterization in the United States." *Proc., 6th Int. Landfill Symp.*, Sardinia, Italy, 253–261.
- Schrefler, B. A., Zhan, X., and Simoni, L. (1995). "A coupled model for water flow, airflow, and heat flow in deformable porous media." *Int. J. Numer. Methods Heat Fluid Flow*, 5, 531–547.
- Senior, E., and Balba, M. T. M. (1990). "Refuse decomposition." *Microbiology of landfill sites*, E. Senior, ed., CRC, Boca Raton, Fla., 17–57.
- Sowers, G. F. (1973). "Settlement of waste disposal fills." *Proc., 8th Int. Conf. on Soil Mechanics and Foundation Engineering*, Moscow, Russia, Vol. 2, 207–210.
- Stearns, R. P. (1987). "Settlement and gas control: Two key post-closure concerns." *Waste Age*, 18(4), 55–60.
- Suklje, L. (1969). *Rheological aspects of soil mechanics*, Wiley-Interscience, London.
- Tchobanoglous, G., Theisen, H., and Vigil, S. A. (1993). *Integrated solid waste management*, McGraw-Hill, New York.
- Wall, D. K., and Zeiss, C. (1995). "Municipal landfill biodegradation and settlement." *J. Environ. Eng.*, 121(3), 214–224.
- Yen, B. C., and Scanlon, B. (1975). "Sanitary landfill settlement rates." *J. Geotech. Eng. Div., Am. Soc. Civ. Eng.*, 101(5), 475–487.
- Yoshikuni, H., Kusakabe, O., Hirao, T., and Ikegami, S. (1994). "Elasto-viscous modelling of time-dependent behavior of clay." *Proc., 13th Int. Conf. on Soil Mechanics and Foundation Engineering*, New Delhi, India, Vol. 1, 417–420.
- Yoshikuni, H., Kusakabe, O., Okada, M., and Tajima, S. (1995). "Mechanism of one-dimensional consolidation." *Compression and consolidation of clayey soils*, H. Yoshikuni and O. Kusakabe, eds., Balkema, Rotterdam, The Netherlands, 497–504.
- Zehnder, A., and Brock, T. D. (1979). "Methane formation and methane oxidation by methanogenic bacteria." *J. Bacteriol.*, 137(1), 420–432.